Cell Reports
Methods

Report

Refined culture conditions with increased physiological relevance uncover oncogene-dependent metabolic signatures in Ewing sarcoma spheroids

Graphical abstract

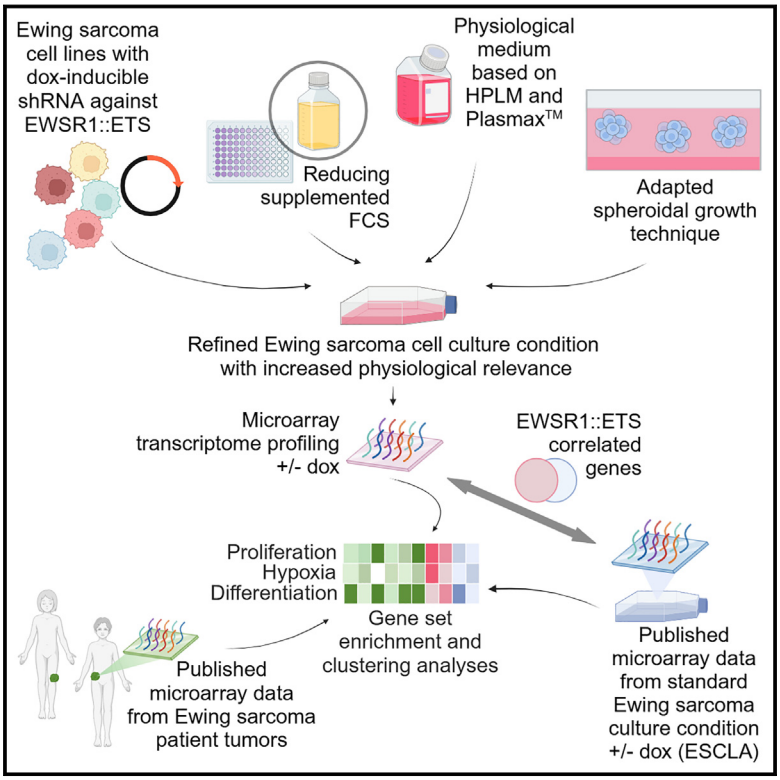

Highlights

- Simple Ewing sarcoma (EwS) cell culture method with increased physiological relevance
- Minimal necessary fetal calf serum supply for EwS cell line proliferation
- Improved transcriptional reflection of proliferation, hypoxia, and differentiation
- EWSR1::ETS transcriptional activity in refined versus standard EwS culture condition

Authors

A. Katharina Ceranski, Martha J. Carreño-Gonzalez, Anna C. Ehlers, ..., Florencia Cidre-Aranaz, Almut Schulze, Thomas G.P. Grünewald

Correspondence

t.gruenewald@kitz-heidelberg.de

In brief

Ceranski et al. report on a refined Ewing sarcoma cell culture method with increased physiological relevance that is technically simple and cost efficient. The enhanced *in vitro* modeling has broad applicability for improving the validity of experimental results.

Ceranski et al., 2025, Cell Reports Methods *5*, 100966
February 24, 2025
https://doi.org/10.1016/j.crmeth.2025.100966

CellPress

Cell Reports Methods

CellPress
OPEN ACCESS

Report

Refined culture conditions with increased physiological relevance uncover oncogene-dependent metabolic signatures in Ewing sarcoma spheroids

A. Katharina Ceranski,[1,2,3,4] Martha J. Carreño-Gonzalez,[1,2,3] Anna C. Ehlers,[1,2,3,4] Kimberley M. Hanssen,[1,2,3] Nadine Gmelin,[1,2,3] Florian H. Geyer,[1,2,3,4] Zuzanna Kolodynska,[1,2,3] Endrit Vinca,[1,2,3,4] Tobias Faehling,[1,2,3,4] Philipp Poeller,[5,6] Shunya Ohmura,[1,2,3] Florencia Cidre-Aranaz,[1,2,3] Almut Schulze,[5] and Thomas G.P. Grünewald[1,2,3,7,8,*]

[1]Hopp-Children's Cancer Center (KiTZ) Heidelberg, Heidelberg, Germany
[2]Division of Translational Pediatric Sarcoma Research, German Cancer Research Center (DKFZ), German Cancer Consortium (DKTK), Heidelberg, Germany
[3]National Center for Tumor Diseases (NCT), NCT Heidelberg, DKFZ and Heidelberg University Hospital, Heidelberg, Germany
[4]Faculty of Medicine, Heidelberg University, Heidelberg, Germany
[5]Division of Tumor Metabolism and Microenvironment, German Cancer Research Center (DKFZ), German Cancer Consortium (DKTK), and DKFZ-ZMBH Alliance, Heidelberg, Germany
[6]Faculty of Biosciences, Heidelberg University, Heidelberg, Germany
[7]Institute of Pathology, Heidelberg University Hospital, Heidelberg, Germany
[8]Lead contact
*Correspondence: t.gruenewald@kitz-heidelberg.de
https://doi.org/10.1016/j.crmeth.2025.100966

MOTIVATION Cell culture remains the main platform for modeling Ewing sarcoma (EwS) for research purposes. Yet, concerns exist about the limitations of standard *in vitro* techniques to adequately reflect physiological conditions. In this study, we refined EwS cell culture conditions to increase modeling capacity while ensuring practical and cost-effective handling, thereby broadening their applicability within the scientific community.

SUMMARY

Ewing sarcoma (EwS) cell line culture largely relies on standard techniques, which do not recapitulate physiological conditions. Here, we report on a feasible and cost-efficient EwS cell culture technique with increased physiological relevance employing an advanced medium composition, reduced fetal calf serum, and spheroidal growth. Improved reflection of the transcriptional activity related to proliferation, hypoxia, and differentiation in EwS patient tumors was detected in EwS cells grown in this refined *in vitro* condition. Moreover, transcriptional signatures associated with the oncogenic activity of the EwS-specific FET::ETS fusion transcription factors in the refined culture condition were shifted from proliferative toward metabolic gene signatures. The herein-presented EwS cell culture technique with increased physiological relevance provides a broadly applicable approach for enhanced *in vitro* modeling relevant to advancing EwS research and the validity of experimental results.

INTRODUCTION

Ewing sarcoma (EwS) is an aggressive pediatric bone and soft tissue cancer that is genetically characterized by *FET::ETS* (members of the FUS/EWSR1/TAF15 family of genes fused to an E26 transformation specific [ETS] transcription factor) fusion oncogenes encoding aberrant transcription factors, mostly *EWSR1::FLI1*.[1] The clinical outcome of many patients, especially that of patients with metastatic disease at diagnosis or relapse, remains limited.[1,2] In fact, patients with metastasis or recurrence typically have <30% overall survival rates.[1,2] There is consensus in the scientific community that preclinical EwS disease models with enhanced physiological relevance are needed, which may, in turn, lead to the identification of more effective therapies.[3–5] The most common preclinic EwS tumor model involves the culture of EwS cell lines in standard techniques, employing a two-dimensional (2D) monolayer setup and traditional cell culture media.[6] However, 2D monolayer culture does not represent the architectural and mechanical aspects of the EwS physiological tumor niche and has been identified to limit the translatability of preclinical research advances into improved therapies for patients with EwS.[7,8] Consequently, various 3D cell culture

techniques, advanced scaffold modeling of the bone extracellular matrix (ECM), flow perfusion techniques, and microfluidic systems have been introduced to improve EwS model accuracy.[3–5,8] Other approaches for more accurate preclinic EwS models include the genetic engineering of EwS cells from mesenchymal stem cells,[9] the use of various types of xenografted animal models,[10,11] and the attempt to create genetically engineered mouse models of EwS, which has not been successful until today.[12] Yet, from a practical standpoint, the complexity of any experimental technique will largely determine its experimental throughput, cost effectiveness, broad applicability, and efforts needed for data acquisition.[4,13] Besides the improvements addressing the architectural aspects of the standard EwS cell culture technique, evidence suggests that physiological cell culture media, such as human plasma-like medium (HPLM)[14] and Plasmax,[15] are essential to enhance the fidelity of *in vitro* cultures.[6,16–18] Yet, physiological cell culture media[14,15] have not been implemented for the culture of EwS cell lines until now. Furthermore, although it is well known that additives such as fetal calf serum (FCS) introduce nutrients, growth factors, and hormones at unknown concentrations to the culture medium,[6,18–20] they are typically applied in high and empiric concentrations, which can compromise the reproducibility of experiments. In fact, little is known about whether EwS cell culture could also be feasible at reduced FCS concentrations that would better comply with the 3R principles (reduction, refinement, and replacement), thereby contributing to the promotion of animal welfare in the experimental space.[19,20]

In this paper, we present a refined EwS cell culture condition with increased physiological relevance that is yet simple, inexpensive, and amenable to large-scale use. We chose a spheroid approach[21] and applied a physiologic medium based on the formulations of HPLM[14] and Plasmax,[15] which mimic nutrient concentrations observed in the human plasma, as well as carefully adapted reduced FCS concentrations to increase the modeling relevancy of the EwS cell culture. Using transcriptome profiling, we show that this refined culture condition better mimics the transcriptional activity related to proliferation, hypoxia, and differentiation in EwS patient tumors. Moreover, we demonstrate that the refined culture condition has a pervasive effect on the baseline transcriptomes of EwS cells and significantly impacts the transcriptional outputs of EWSR1::ETS fusion oncogenes.

RESULTS

Establishing a refined culture condition for EwS cell lines with increased physiological relevance

To improve the physiological relevance of the EwS standard culture condition, we addressed three technical aspects in the refined EwS culture condition: medium composition, FCS concentration, and growth architecture (Figure 1A). In the first step, two established physiological media, HPLM[14] and Plasmax,[15] were combined to generate a physiological medium, hereafter called HPLMax (Figure 1B; Table S1; see STAR Methods). EwS cell lines were considered adapted after 4 weeks of culturing in HPLMax and were then phenotypically characterized. In a second step, to evaluate the minimal necessary FCS concentration that did not compromise EwS cell viability, we performed a resazurin proliferation assay for five selected EwS cell lines cultured in Roswell Park Memorial Institute (RPMI) 1640 medium with FCS concentrations ranging from 10% (standard) to 1%. The human EwS cell lines A-673, MHH-ES-1, SK-N-MC, TC-71 (all *EWSR1::FLI1* positive), and TC-106 (*EWSR1::ERG* positive) were selected for study since they are widely used in EwS research and reflect the two major *EWSR1::ETS* fusions found in ~95% of patients.[1] Of note, all cell lines were previously engineered to harbor doxycycline (dox)-inducible short hairpin RNAs (shRNAs) to target the respective *FET::ETS* fusions.[22] Moreover, all cell line models were characterized in depth beforehand via multi-omics analyses,[22] and information on their status concerning frequent EwS secondary mutations[1,23,24] is given in Figure S1A. Interestingly, for all five tested EwS cell lines, FCS supplementation could be reduced to 7% without significantly decreasing their proliferation (Figures 1C and S1B). In fact, 7% FCS supplementation resulted in even slightly accelerated proliferation for some cell lines (SK-N-MC/TR/shEF1 and TC-71/TR/shEF1; see also Figure S1B). While we have chosen 7% FCS because this was the concentration under which we did not detect a significantly reduced proliferation for all cell lines tested (Figure 1C), it should be noted that some EwS cell lines continued to proliferate even under way lower FCS concentrations, such as SK-N-MC/TR/shEF1 cells, which did not display a significantly reduced signal in the resazurin assay as compared to 10% FCS even in 2% FCS (Figure 1B). The 7% FCS optimized condition was further validated by manual cell counting using standardized hemocytometers and trypan blue exclusion methods in both RPMI 1640 medium and the physiological HPLMax medium: all EwS cell lines demonstrated no significant change of their doubling time in either medium when changing the FCS concentration from 10% to 7% (Figure 1D). Moreover, manual cell counting demonstrated no notable change in EwS cell viability with 10% versus 7% FCS supplementation in either medium (Figure 1E). We concluded that a 7% FCS supplementation is optimal for these EwS cell lines to provide the required growth factors while allowing a 30% reduction of this animal product and its entailed drawbacks for experimentation.[6,18–20] Although proliferation rates of all EwS cell lines remained stable within both media (RPMI 1640 medium and HPLMax) despite the 30% decrease in FCS supplementation (Figure 1D), we did observe a slower proliferation in the five EwS cell lines when comparing the doubling time in HPLMax to RPMI 1640 medium under an equal medium exchange frequency (Figure 1D). This result is consistent with the fact that conventional media were designed to maximize the growth rates of cultured cells[14,15] and similar results have been previously reported for the proliferation of hematological and epithelial cancer cell lines in HPLM.[14,25] Concerning the viability of the five EwS cell lines, similar dead cell counts were found in RPMI 1640 medium and HPLMax (Figure 1E). Regarding the EwS cell line morphology, no striking changes were observed *in vitro* between culture in RPMI 1640 medium and HPLMax (Figures 1F and S1C). Lastly, the traditional 2D monolayer culture was replaced with a spheroid approach (Figure 1G) by adjusting a published protocol for agar-coated, low-attachment spheroid culture[21] (see STAR Methods). This allows for optimized mimicking of the tumor architecture (Figure 1G), cell-cell

CellPress
OPEN ACCESS

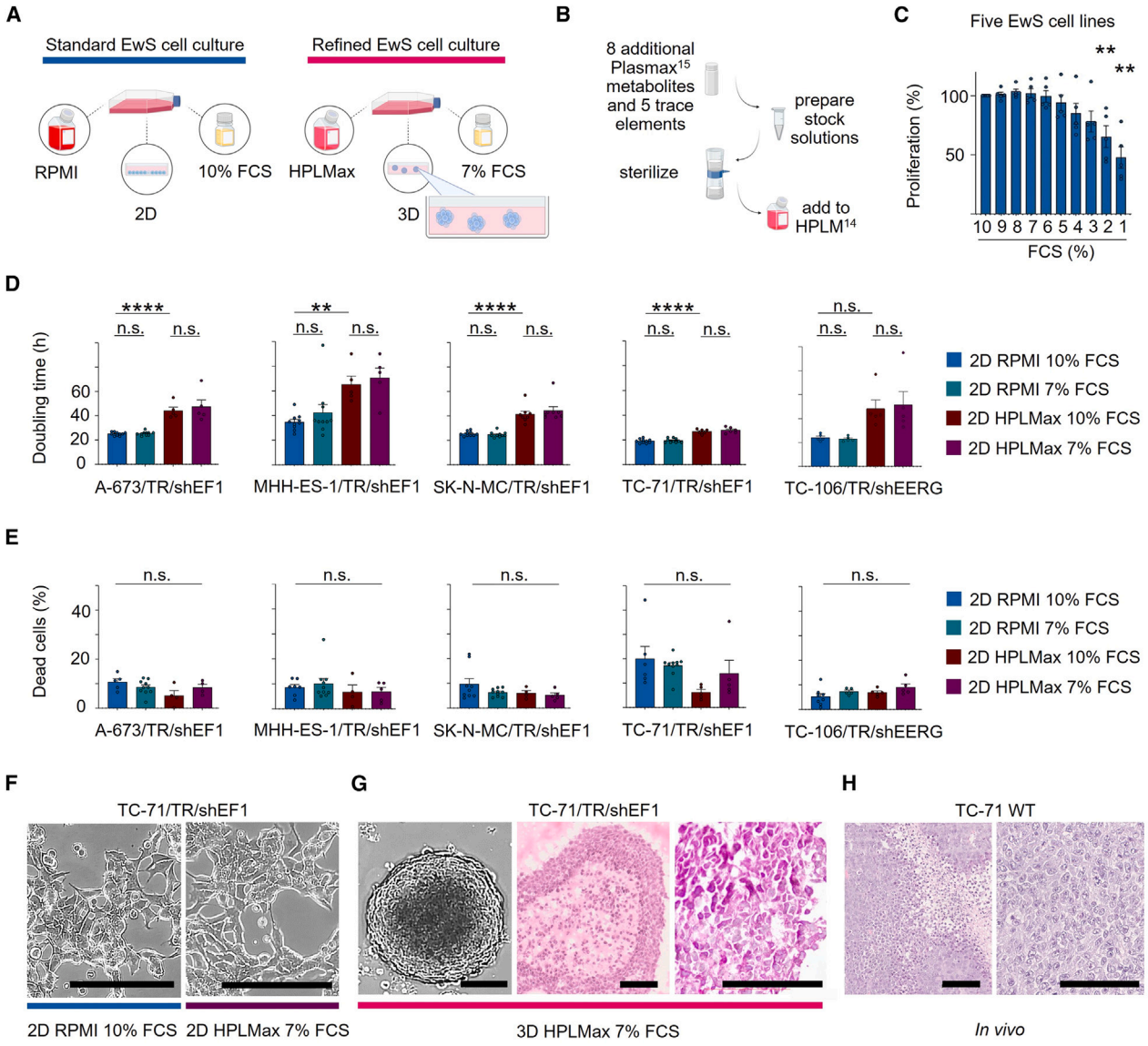

Figure 1. Establishing a refined culture condition for EwS cell lines with increased physiological relevance

(A) Overview on the EwS *in vitro* standard and refined techniques.

(B) Workflow to create HPLMax (see also Table S1).

(C) Proliferation assessment by resazurin cell viability assays in EwS cell lines in RPMI 1640 medium with FCS supplementation from 10% to 1%. Values were normalized to the proliferation in 10% FCS. Pooled data of five representative cell lines are shown, with each dot representing $n \geq 5$ biologically independent replicates of one cell line. Vertical bars represent means and whiskers the standard error of the mean (SEM). $^{**}p < 0.01$ and $^{***}p < 0.001$ (see also Figure S1B).

(D) Doubling time of five EwS cell lines in RPMI 1640 medium and 10% FCS (left bar), RPMI 1640 medium and 7% FCS (second bar from left), HPLMax and 10% FCS (second bar from right), and HPLMax and 7% FCS (right bar) assessed by trypan blue counting of viable cells. Each dot represents a single biologically independent experiment. Vertical bars represent means and whiskers the SEM. One-way ANOVA with Tukey's multiple comparisons test; $^{**}p < 0.01$ and $^{****}p < 0.0001$; n.s., non-significant.

(E) Dead cell counts using trypan blue exclusion method in RPMI 1640 medium and 10% FCS (left bar), RPMI 1640 medium and 7% FCS (second bar from left), HPLMax and 10% FCS (second bar from right), and HPLMax and 7% FCS (right bar). Values are the percentage of the total cell count (viable and dead cells) in the respective sample. Each dot represents a single biologically independent experiment. Vertical bars represent means and whiskers the SEM. One-way ANOVA with Tukey's multiple comparisons test; n.s., non-significant.

(F) Bright-field microscopy images of TC-71/TR/shEF1 cell lines grown in RPMI 1640 medium and 10% FCS (left) and in HPLMax and 7% FCS (right). Scale bars: 200 μm, 10× magnification (see also Figure S1).

(G) TC-71/TR/shEF1 spheroids grown in agar-coated T25 flasks with HPLMax and 7% FCS for 8 days. Light microscopy image (left), scale bar: 125 μm, in 4× magnification. Hematoxylin and eosin (H&E) staining of TC-71/TR/shEF1 spheroids grown as described above in 20× magnification, scale bar: 100 μm (middle), and 40× magnification (right), scale bar: 100 μm.

(H) H&E staining of mice *in vivo* xenografts of TC-71 wild-type cells in 20× magnification, scale bar: 100 μm (left), and 40× magnification (right), scale bar: 100 μm.

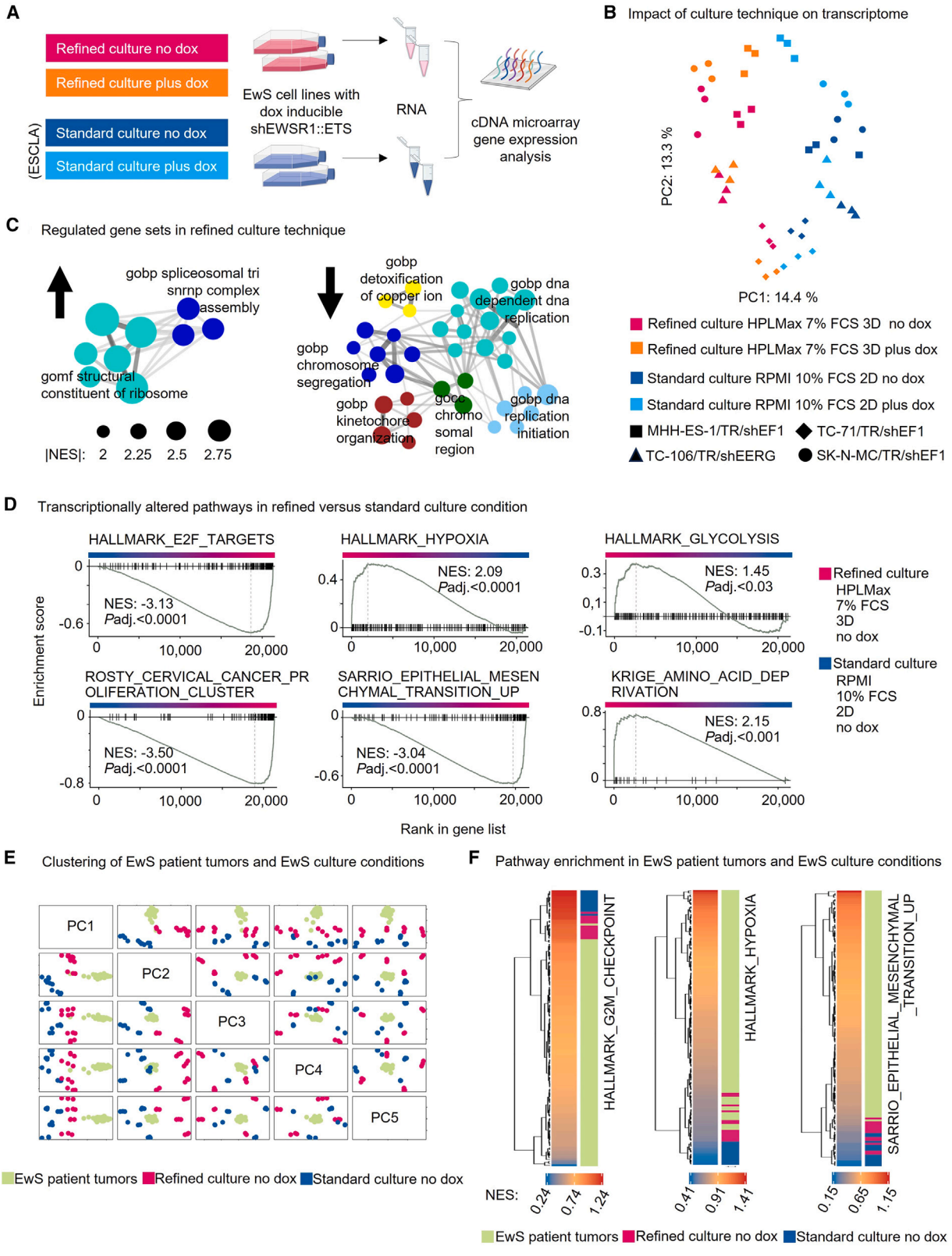

(legend on next page)

interactions, and spatial gradients of oxygen[26] and nutrients,[4] which are all essential components of the tumor microenvironment.[4,27] The architectural fidelity of the EwS spheroids cultured in the refined condition could be demonstrated by histological comparison with an *in vivo* EwS xenograft (Figure 1G).

The refined EwS culture condition preserves cell line characteristics but alters transcriptional programs related to proliferation, differentiation, and metabolism

To further characterize the EwS cells in the refined culture condition and validate this setup, we performed DNA microarray gene expression analyses in four EwS cell lines (MHH-ES-1/TR/shEF1, SK-N-MC/TR/shEF1, TC-71/TR/shEF1, and TC-106/TR/shEERG) that enable a dox-inducible and shRNA-mediated knockdown of either EWSR1::FLI1 or EWSR1::ERG, respectively.[22] An experimental overview is given in Figure 2A. Briefly, the Ewing Sarcoma Cell Line Atlas (ESCLA) transcriptome experiment from our laboratory in standard culture conditions[22] was recapitulated in the refined cell culture with/without the addition of dox for 96 h. Gene expression data were generated on the same platform (human Affymetrix Clariom D arrays), jointly preprocessed, and normalized with the former data[22] to generate a harmonized dataset for a direct comparison of refined and standard culture conditions. Exploratory data analysis using principal-component analysis (PCA) demonstrated that the captured variation between all samples was mainly driven by three aspects (Figures 2B, S2A, and S2B): the employed culture condition (PC1), the specific characteristics of the individual cell lines (PC2–PC4), and the dox-dependent *EWSR1::ETS* expression levels (PC5). This illustrates that the applied culture technique fundamentally affects transcriptional programs of EwS cell lines, yet their principal characteristics are preserved in the refined setup. Next, to further explore the effects of the culture conditions on baseline RNA transcription, we focused on samples without *EWSR1::ETS* knockdown (no dox). Pre-ranked fast gene set enrichment analysis (fGSEA) with differentially expressed genes (DEGs) between the refined and standard culture conditions followed by weighted gene correlation network analysis (WGCNA) uncovered reduced cell cycle- and proliferation-associated signatures as well as enrichment of ribosomal, translational, and spliceosomal processes in the physiologically refined condition (Figures 2C and 2D; Table S2). Furthermore, we observed a strong dysregulation of canonical hallmark and generic gene signatures involved in the regulation of differentiation (epithelial-to-mesenchymal transition [EMT]), hypoxia, and metabolism in the refined setup (Figure 2D). These data are in keeping with the results from the functional *in vitro* proliferation assays (Figure 1G) and the oxygen gradients that are a key feature of spheroid cultures.[4,26] Altogether, these results indicate that the refined culture condition does not alter principal EwS cell line characteristics but impacts transcriptional programs related to proliferation, differentiation, metabolism, and hypoxia.

Lastly, we compared the microarray-based gene expression profiles from the EwS cells in standard and refined culture conditions (both no dox; Figure 2A) with those from 50 EwS patient tumors.[28] PCA revealed that in PC1 and PC2, which account for the largest proportion of variance (Figure S2C), gene expression profiles of EwS cells from the refined condition clustered closer with EwS tumors than the profiles of EwS cells from the standard culture (Figure 2E). However, this pattern was not maintained across PC2–PC5 (Figure 2E). To quantify the concordance between the two *in vitro* conditions and the tumor samples, we used pairwise Pearson correlation-based distance calculations between all samples. While the overall distances between the tumor samples and EwS cells from the refined condition were significantly smaller than those between tumor samples and EwS cells from the standard condition (one-sided Wilcoxon test of two sets of pairwise distances, $p < 9.266951e{-}43$), the change in the absolute values was less prominent. Hence, we hypothesized that the refinements made to the EwS standard culture condition enhanced the physiological relevance of this model for specific pathophysiological aspects rather than globally for any aspect. To uncover which might be the precise features of EwS patient tumors that are better mimicked in the refined condition, we conducted single-sample GSEAs (ssGSEAs) with the gene expression data from both EwS *in vitro* conditions and an extended and well-curated EwS tumor cohort[29] (Figures 2F and S2D). The normalized enrichment scores (NESs) of transcriptional signatures related to cell cycle progression, hypoxia, and EMT of EwS patient tumors were better represented by EwS cells grown in the refined condition (Figures 2F and S2D). We also observed an improved reflection of a signature comprising the top 1,000 most highly expressed genes in EwS patient tumors in the refined versus standard

Figure 2. The refined EwS culture condition preserves cell line characteristics but alters transcriptional programs related to proliferation, differentiation, metabolism, and hypoxia

(A) Experimental workflow to generate transcriptome datasets for EwS cell lines in refined culture conditions (pink and orange). The same experiment was previously performed for the Ewing Sarcoma Cell Line Atlas (ESCLA) in standard culture conditions by Orth et al.[22] (blue and light blue). Data were analyzed via joint processing (see STAR Methods).

(B) Principal-component analysis (PCA) of the normalized data from (A) revealing captured variation driven by culture condition (PC1) and cell line characteristics (PC2). For captured variation by PC3–PC5, see Figures S2A and S2B.

(C) Weighted correlation network analysis (WGCNA) based on pre-ranked fast gene set enrichment analysis (fGSEA) of differentially expressed genes (DEGs) from (A) using the average rank of expression fold change (FC). Displayed network analyses were based on significant gene sets with a maximum false discovery rate (|FDR|) of 0.05 and a minimal normalized enrichment score (|NES|) of 2. See also Table S2.

(D) Enrichment plots from fGSEA of DEGs in refined versus standard condition from (A). *p*adj, Bonferroni-adjusted *p* value. C2 and hallmark gene sets from the Human MSigDB Collections. See also Table S2.

(E) Pairwise correlation plot based on PCA of gene expression profiles from (A) ($n = 12$ in each condition) and EwS primary tumors ($n = 50$)[28] after preprocessing, normalization, and batch correction for both datasets. See also Figure S2C.

(F) Heatmaps depicting NESs of single-sample GSEA (ssGSEA) with gene expression profiles from (A) ($n = 12$ in each condition) and EwS primary tumors ($n = 117$).[29] Signatures were derived from C2 and hallmark gene sets from the Human MSigDB Collections. See also Figure S2D.

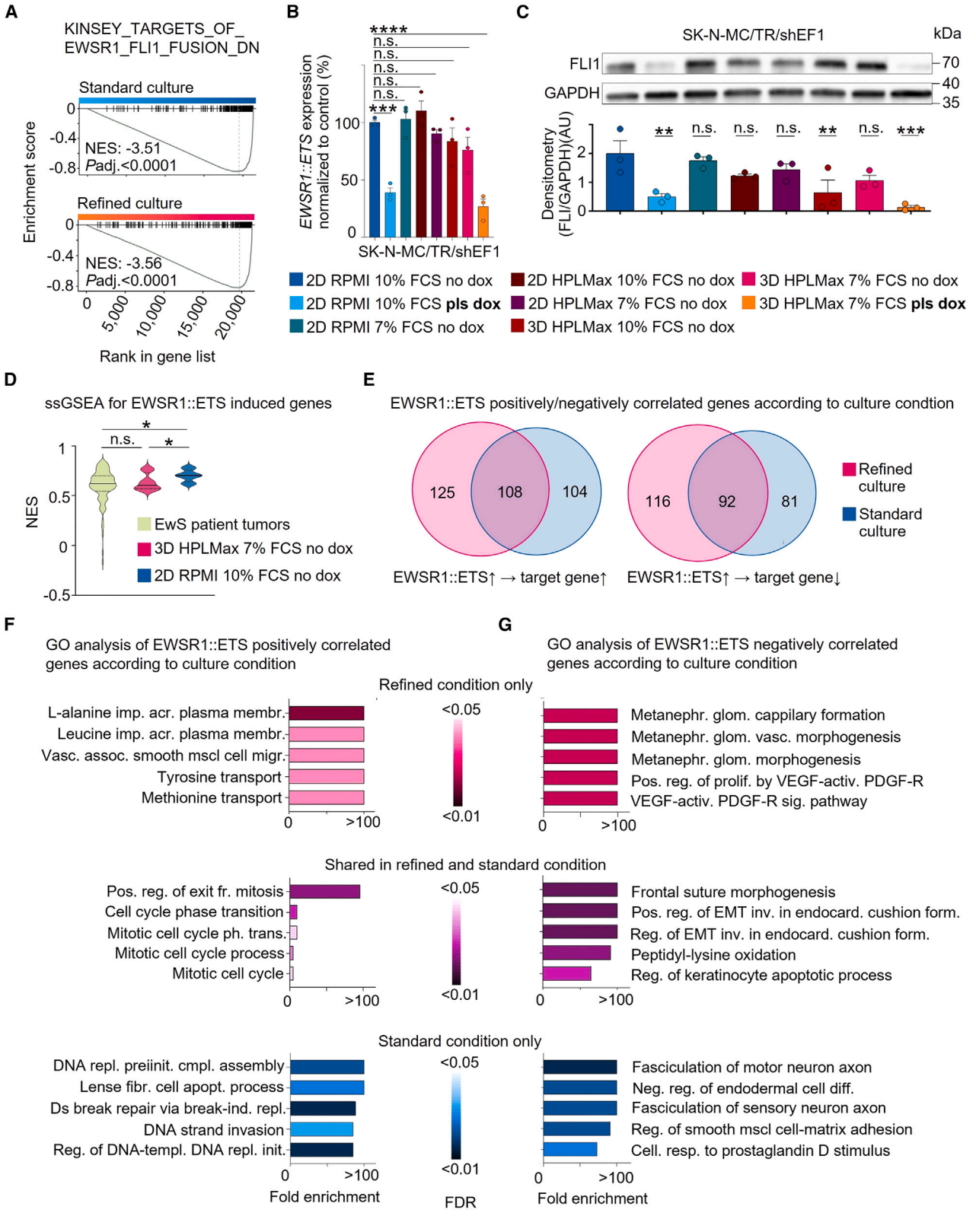

(legend on next page)

EwS culture conditions (Figure S2D). Collectively, these results suggest that the transcriptomes of EwS cells cultured in the refined condition better represent EwS patient tumor transcriptomes regarding signatures for proliferation, hypoxia, and EMT.

The refined EwS culture condition shapes the transcriptional output of EWSR1::ETS

Since oncogenic EWSR1::ETS transcription factors are the most prominent genetic characteristic of EwS,[1] we subsequently investigated their transcriptional activity in the refined culture condition in comparison to the standard condition. In both culture conditions, dox-induced and shRNA-mediated knockdown of the fusions for 96 h resulted in a strong downregulation of a well-established EWSR1::ETS-related gene signature[30] ("Kinsey_targets_of_EWSR1::FLI1-fusion_down," NES < -3; Figure 3A), which was in agreement with the efficient knockdown of the fusion at the mRNA and protein levels, as shown in Figures 3B and 3C, for the representative EWSR1::FLI1-positive cell model SK-N-MC/TR/shEF1. Similar observations were made in the EWSR1::ERG-positive cell model TC-106/TR/shEERG (Figure S3). Of note, the EWSR1::ETS mRNA and protein levels in the refined culture condition (no dox) did not exhibit remarkable changes compared to the standard culture condition in either cell line (no dox; Figures 3B, 3C, and S3), suggesting that the above-described transcriptional alterations regarding cell proliferation, hypoxia, and differentiation in the refined culture setup are not primarily due to altered EWSR1::ETS expression levels. To further characterize the EWSR1::ETS transcriptional activity in our refined cell culture condition, we performed ssGSEA with our previously established core signature of EWSR1::ETS-induced genes[22] on transcriptome data of the EwS cell line samples in both culture conditions (no dox) and the EwS patient cohort.[29] Strikingly, as shown in Figure 3D, the mean NESs of the EwS cells from the refined condition better reflected the mean NESs of primary EwS tumors (no significant difference, $p = 0.51$) than those of the standard condition ($p = 0.035$).

Next, we compared differentially regulated genes under EWSR1::ETS knockdown in the two culture conditions for shared EWSR1::ETS positively correlated and EWSR1::ETS negatively correlated genes in both conditions as well as genes uniquely regulated in either culture condition. Strikingly, while there were notable overlaps in EWSR1::ETS-regulated genes between the two conditions, there was also a large proportion (~50%) of genes specific to each culture technique (Figure 3E). Among the EWSR1::ETS-regulated genes that were shared in both cell culture conditions, Gene Ontology (GO) analysis revealed that upregulated gene sets in EWSR1::ETS-high conditions (no dox) were predominantly associated with cell cycle progression (Figure 3F; Table S3). Similarly, proliferation signatures were overrepresented among EWSR1::ETS-correlated genes exclusively in standard cell culture conditions (Figure 3F; Table S3), which corresponds to previous reports that linked higher EWSR1::ETS expression in EwS to increased proliferation.[31,32] Most interestingly, genes that were EWSR1::ETS correlated exclusively in the refined culture condition were primarily categorized by GO analysis as participating in amino acid membrane transport (e.g., L-alanine and leucine import across plasma membrane, GO: 1904273 and 0098713) (Figure 3F; Table S3). Hence, this suggests that EWSR1::ETS facilitate nutrient transport, which is not apparent under the supraphysiological nutrient concentrations present in traditional cell culture media. For EWSR1::ETS negatively correlated genes, GO analysis retrieved differentiation processes that were reduced through the upregulation of EWSR1::ETS in genes overlapping between the two medium conditions as well as those unique to either condition (Figure 3G; Table S3). This reflects the known role of EWSR1::ETS in maintaining a dedifferentiated state.[31] Collectively, our data show that the activity of EWSR1::ETS fusions in EwS cell lines is shifted under cell culture conditions with increased physiological relevance from a hyperproliferative state toward enhanced amino acid transport while maintaining a dedifferentiated state. As the reliance on extracellular nutrients under nutrient limiting conditions can be an exploitable vulnerability in cancer cells,[18] these findings may have significant implications for future EwS research that aims for accurate discoveries of EWSR1::ETS-regulated genes and drug targets.[33]

Cell culture conditions may influence expression of commonly used HKGs

It is well established that specific experimental conditions (e.g., cell culture techniques) can influence the expression levels of

Figure 3. The refined EwS culture condition shapes the transcriptional output of EWSR1::ETS

(A) Enrichment plots from fGSEA of DEGs between EWSR1::ETS-high versus EWSR1::ETS-low (as indicated by color)-expressing EwS cell lines in standard (top) and refined (bottom) conditions. C2 gene set from the Human MSigDB Collections.

(B) *EWSR1::ETS* expression in SK-N-MC/TR/shEF1 cultured in eight different culture conditions. *GAPDH* served as the HKG, and values are shown as a percentage of *EWSR1::ETS* expression in the standard condition (2D RPMI 1640 medium and 10% FCS, no dox). $n = 3$ biologically independent experiments. Vertical bars represent means and whiskers the SEM. Statistical significance comparisons are to the standard condition. One-way ANOVA with Dunnett's multiple comparisons test; ***$p < 0.001$ and ****$p < 0.0001$; n.s., non-significant.

(C) EWSR1::ETS expression in SK-N-MC/TR/shEF1 in eight different culture conditions. Representative western blot and densitometry values ($n = 3$ biologically independent experiments; AU, area under the curve). GAPDH was used as a housekeeping protein.[22] Vertical bars represent means and whiskers the SEM. Statistical significance comparisons are to the standard condition with one-way ANOVA with Dunnett's multiple comparisons test.

(D) Violin plot of NESs of single-sample GSEA (ssGSEA) on gene expression profiles from Figure 2A ($n = 12$ in each condition) and EwS primary tumors ($n = 117$)[29] with our previously established core signature of EWSR1::ETS-induced genes.[22] Horizontal dashed lines represent the first and third quartiles (Q1 and Q3), and solid lines indicate the median. *$p < 0.05$; n.s., non-significant.

(E) Area-proportional Venn diagram showing overlap of DEGs, defined as having FDR-adjusted $p \leq 0.05$ and $|\log2\ FC| \geq 1.5$, in refined and standard culture conditions. Left side: EWSR1::ETS positively correlated DEGs; right side: EWSR1::ETS negatively correlated DEGs. See also Table S3.

(F) Gene Ontology (GO) analysis of EWSR1::ETS positively correlated DEGs from (E) showing top five enriched GO biological processes for each collection of DEGs. The top row (pink) shows DEGs from refined culture conditions exclusively, the middle row (violet) shows DEGs that are shared in both culture conditions, and the bottom row (blue) shows DEGs from standard culture conditions only. See also Table S3.

(G) Analogously to (F) with EWSR1::ETS negatively correlated DEGs. See also Table S3.

A

Gene	Mean expresison	SD	MFC < 2	Rank Sorted by CV
MT-CO-1	19.37	0.12	yes	1
MT-ND-1	19.45	0.12	yes	2
RN7SK	19.24	0.12	yes	3
…	…	…	…	…
GAPDH	18.94	0.29	yes	34
…	…	…	…	…
RPLP0	17.08	0.91	yes	3320

B

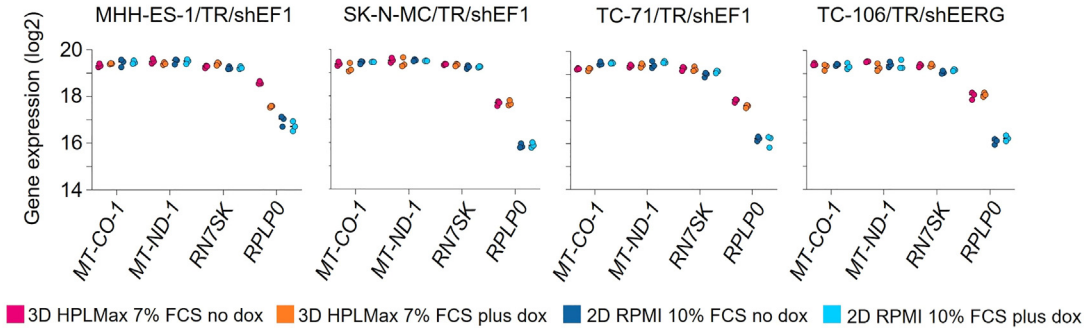

Figure 4. Cell culture conditions may influence the expression of commonly used HKGs

(A) Table of the top three housekeeping gene (HKG) candidates and the routinely used HKGs *GAPDH* and *RPLP0*. HKG candidates were selected through the adapted approach from de Jonge et al.[34] Mean expression value is defined as mean of the expression values of all samples from Figure 2A, including the four different conditions. SD, standard deviation; MFC, maximum FC; CV, coefficient of variation. See also Table S4 and STAR Methods.

(B) Log2-transformed gene expression of HKG candidates from the microarray data in the four EwS cell lines from Figure 2A.

housekeeping genes (HKGs), which may introduce a bias into studies based on real-time qPCR readouts.[34,35] Indeed, when assessing our microarray data, we observed that *ribosomal protein lateral stalk subunit P0* (*RPLP0*), a routinely used HKG in EwS research,[22] exhibited markedly different baseline expression levels between the standard and refined cell culture conditions. To nominate potential HKGs exhibiting minimal variation across cell culture conditions, we employed and adapted an approach described by de Jonge et al.[34] (see STAR Methods). As displayed in Figure 4A, the top three candidate HKGs were the *mitochondrially encoded cytochrome c oxidase I* (*MT-CO1*), *mitochondrially encoded NADH dehydrogenase 1* (*MT-ND1*), and *RNA component of 7SK nuclear ribonucleoprotein* (*RN7SK*), a small nuclear RNA (snRNA). Indeed, these three genes showed little variation as compared to *RPLP0* (Figure 4B). A comprehensive list of potential HKGs is provided in Table S4. These data confirm the rationale that the choice of a suitable HKG must be tailored to the specific cell line and applied cell culture condition.[34,35]

DISCUSSION

In this report, we pursue a practical approach to enhance the physiological relevance of the standard culture technique for EwS cell lines. The refined culture condition was validated through comparative transcriptome analyses of gene expression data from four EwS cell lines cultured in standard[22] and refined conditions as well as from EwS patient tumors.[28,29] These analyses indicated that EwS cell line characteristics, including EWSR1::ETS activity, were preserved between the two culture conditions, while transcriptionally altered signatures in the refined versus standard culture conditions involved cell cycle progression, hypoxia, metabolism, translation, and differentiation (i.e., EMT). Of these, we found that cell cycle progression-, hypoxia-, and EMT-related transcriptional signatures of EwS cells from the refined condition better represented the respective transcriptional activity detected in EwS patient tumors than those from EwS cells grown in the standard condition. Notably, hypoxia is an important component of the EwS tumor microenvironment[27,36] that is relevant for EwS pathophysiology,[9,36] as well as the complex interplay of proliferation and differentiation processes.[1,31,32] Hence, we consider the herein-presented refined culture condition a suitable model for EwS *in vitro* studies, which might be, due to the improved modeling of proliferation, differentiation, and hypoxia, particularly relevant for future studies investigating these processes in EwS pathophysiology.

Our results demonstrate that the employed cell culture conditions influence two aspects relevant to EwS research: (1) transcriptional programs linked to a variety of cellular processes, such as proliferation, translation, differentiation, and metabolism,

and (2) the activity of the EWSR1::ETS oncogenic transcription factors. Regarding the first aspect, our data are consistent with previously published studies in that metabolism and proliferation are frequently altered when cells are cultured in physiological media.[14,17,37] This is also reflected in our data by the upregulation of ribosomal and translational processes when changing from standard to refined EwS cell culture conditions since translation and metabolism are tightly correlated in both normal and cancer cells.[38,39] Consequently, it is intriguing to further characterize EwS features in the refined and physiologically relevant condition by means of extended multi-omics profiling, including the proteomic level.

Concerning the second aspect, our study provides insight into potential alterations of the metabolic landscape in EwS induced by the activity of EWSR1::ETS oncoproteins in a physiologically relevant cell culture model. We hypothesize that the observed altered expression of genes engaged in amino acid membrane transport in physiologic media is necessary to sustain the proliferation of high-EWSR1::ETS-expressing EwS cell lines[31,32] in physiological media. Interestingly, the transcriptional regulation of genes involved in amino acid metabolic pathways in the context of proliferation in physiological media has already been described in other tumor entities.[17,37] Our data support the idea that altered metabolic pathways related to amino acid abundance are a characteristic trait of proliferating cells in physiological media. To fully characterize which amino acids and metabolic pathways are required for the proliferation of high-EWSR1::ETS-expressing EwS cell lines, further studies on the interaction of FET::ETS oncogenes and the metabolism in EwS cells are needed. Finally, our data illustrate that the applied cell culture technique, as a part of the general experimental conditions, can influence the expression levels of routinely used HKGs[34,35]—as was the case for *RPLP0*[22] in this study.

In summary, our work underlines the necessity to improve the physiological relevance of cell culture conditions, provides a pragmatic and cost-effective approach for the EwS field to overcome typical barriers for establishing these, and contributes a transcriptome dataset generated in refined *in vitro* conditions as a valuable resource to the EwS research community.

Limitations of the study

The technical limitations of our refined culture technique for EwS cell lines involve primarily the natural restrictions of any spheroid-based technique. The ability of tumor cells to spontaneously form spheroids when cultured in low-attachment conditions is a prerequisite for this approach.[4] Further restrictions include the variability in size and diameter between individual spheres; if cultured on flat-bottom surfaces, the lack of a vasculature or dynamic flow system; and, in our experimental setup, the absence of ECM components.[4] On that account, alternative methods have been developed to mimic the interactions of EwS cells with the ECM and mechanical forces.[3–5,8] These techniques could also be combined with physiological media[14,15] and the reduced FCS concentration that we propose in this report.

Limitations to our intention to increase the physiological relevance by means of refining the standard EwS cell culture condition were mirrored in the relatively small improvements in the overall comparison of the *in vitro* gene expression profiles with EwS patient tumors. This might be explained in part by the systematic discrepancies between cancer cell lines employed for *in vitro* studies and tumor cells thriving in the human body.[40] While we could detect an improved modeling for some physiological processes such as proliferation, differentiation, and hypoxia in the refined EwS culture, this did not apply for all pathophysiological aspects of EwS patient tumors. These considerations should guide the selection of appropriate *in vitro* models for future EwS studies.

Some of the limitations discussed above are a result of our intention to keep the cell culture technique simple, feasible, and cost effective. It is due to this motivation that our refined cell culture condition for EwS cell lines is amenable to routine and large-scale use and especially suitable for bulk analyses in a setting with increased physiological relevance.

RESOURCE AVAILABILITY

Lead contact

Requests for resources of this article and any additional information should be directed to the lead contact, Thomas G.P. Grünewald (t.gruenewald@dkfz-heidelberg.de)

Materials availability

This study did not generate new unique reagents.

Data and code availability

- Original Affymetrix transcriptome profiling data have been deposited at the GEO and are publicly available under the accession code GEO: GSE270118.
- Microscopy data and western blot images reported in this paper will be shared by the lead contact upon request.
- This study did not generate new original code.
- Any additional information required to reanalyze the data reported in this paper is available from the lead contact upon request.
- In addition, Affymetrix microarray data from our published Ewing Sarcoma Cell Line Atlas (ESCLA)[22] (accession code: GSE176190) as well as an Affymetrix microarray dataset from multiple human tumor samples including EwS[28] and an Affymetrix microarray dataset from an EwS patient tumor cohort[29] (accession code GSE34620) were used for comparison.

ACKNOWLEDGMENTS

We thank Felina Zahnow, Stefanie Kutschmann, and Sabrina Knoth for their excellent technical assistance. We thank Angelina Yershova, Jia Xiang Jin, and Dr. Jing Li for fruitful discussions and advice during the project. We thank the Microarray Core Facility, German Cancer Research Center (DKFZ), for providing excellent expression profiling services. We thank Gaby Blaser, Claudia Schmidt, and the team from the DKFZ Light Microscopy Core Facility for valuable technical support. The laboratory of T.G.P.G. is supported by grants from the Matthias Lackas Foundation, the Dr. Leopold and Carmen Ellinger Foundation, the Deutsche Forschungsgemeinschaft (DFG 458891500), the Dr. Rolf M. Schwiete Foundation (2021-007 and 2022-031), the German Cancer Aid (DKH-7011411, DKH-70114278, DKH-70115315, and DKH-70115914), the SMARCB1 Association, the Ministry of Education and Research (BMBF; SMART-CARE and HEROES-AYA), the KiKa Foundation, the Fight Kids Cancer Foundation (FKC-NEWtargets), the KiTZ Foundation in memory of Kirstin Diehl, the Kitz-PMC Twinning Program, the German Cancer Consortium (DKTK, PRedictAHR), and the Barbara and Wilfried Mohr Foundation. The laboratory of T.G.P.G. is co-funded by the European Union (ERC, CANCER-HARAKIRI, 101122595). The views and opinions expressed are, however, those of the authors only and do not necessarily reflect those of

the European Union or the European Research Council. Neither the European Union nor the granting authority can be held responsible for them. A.C.E., F.H.G., T.F., and E.V. were supported by a scholarship from the German Cancer Aid and the German Academic Scholarship Foundation. E.V. and T.F. were additionally supported by a scholarship from the Heinrich F.C. Behr Foundation and E.V. by the Rudolf and Brigitte Zenner Foundation. K.M.H. was supported by a fellowship from the Alexander von Humboldt Foundation.

AUTHOR CONTRIBUTIONS

A.K.C., M.J.C.-G., N.G., Z.K., and E.V. performed *in vitro* experimental assays. P.P. and A.S. provided the HPLMax medium composition and fabrication protocol and gave experimental advice. A.K.C. and M.J.C.-G. prepared HPLMax. K.M.H. and N.G. performed western blots, and K.M.H. gave advice on metabolic aspects of the culture conditions. F.C.-A. and S.O. contributed to histology analyses. A.C.E. performed bioinformatic analyses that are the basis for Figures 2B–2E, 3A, 3B, 3F, 3G, 4A, and S2A–S2C. F.H.G. performed bioinformatic analyses that are the basis for Figures 2F, 3E, and S2D. A.K.C., A.C.E., F.H.G., M.J.C.-G., and T.G.P.G. performed statistical analyses. T.F. provided and analyzed an additional dataset to cross-check for HKG candidates. A.K.C., A.C.E., F.H.G., and T.G.P.G. prepared the figures. A.K.C. and T.G.P.G. wrote and revised the manuscript. A.K.C., M.J.C.-G., and T.G.P.G. designed the experimental assays. T.G.P.G. conceived and supervised the study and provided the laboratory infrastructure and financial support. All authors read and approved the manuscript.

DECLARATION OF INTERESTS

The authors declare no competing interests.

STAR★METHODS

Detailed methods are provided in the online version of this paper and include the following:

- KEY RESOURCES TABLE
- EXPERIMENTAL MODEL AND STUDY PARTICIPANT DETAILS
  - Provenance of cell lines
  - Culture conditions for cell lines
  - Spheroid seeding
- METHOD DETAILS
  - Fabrication HPLMax
  - Cell lines with *EWSR1::ETS*-knockdown
  - Proliferation assays
  - Spheroid histology
  - RNA extraction and qRT-PCR
  - Western blot
  - Transcriptome analyses
  - Comparison and distance calculations of EwS patient tumor and in vitro gene expression profiles
  - Single sample gene-set enrichment analyses (ssGSEA)
  - Pathway enrichment analysis
  - Identification of HKG candidates in refined and standard EwS culture conditions
- QUANTIFICATION AND STATISTICAL ANALYSIS
  - Statistical analysis and software

SUPPLEMENTAL INFORMATION

Supplemental information can be found online at https://doi.org/10.1016/j.crmeth.2025.100966.

Received: July 12, 2024
Revised: December 23, 2024
Accepted: January 17, 2025
Published: February 7, 2025

REFERENCES

1. Grünewald, T.G.P., Cidre-Aranaz, F., Surdez, D., Tomazou, E.M., de Álava, E., Kovar, H., Sorensen, P.H., Delattre, O., and Dirksen, U. (2018). Ewing sarcoma. Nat. Rev. Dis. Prim. *4*, 5. https://doi.org/10.1038/s41572-018-0003-x.
2. Gaspar, N., Hawkins, D.S., Dirksen, U., Lewis, I.J., Ferrari, S., Le Deley, M.C., Kovar, H., Grimer, R., Whelan, J., Claude, L., et al. (2015). Ewing Sarcoma: Current Management and Future Approaches Through Collaboration. J. Clin. Oncol. *33*, 3036–3046. https://doi.org/10.1200/JCO.2014.59.5256.
3. Munoz-Garcia, J., Jubelin, C., Loussouarn, A., Goumard, M., Griscom, L., Renodon-Cornière, A., Heymann, M.F., and Heymann, D. (2021). In vitro three-dimensional cell cultures for bone sarcomas. J. Bone Oncol. *30*, 100379. https://doi.org/10.1016/j.jbo.2021.100379.
4. Molina, E.R., Chim, L.K., Barrios, S., Ludwig, J.A., and Mikos, A.G. (2020). Modeling the Tumor Microenvironment and Pathogenic Signaling in Bone Sarcoma. Tissue Eng., Part B *26*, 249–271. https://doi.org/10.1089/ten.teb.2019.0302.
5. Lamhamedi-Cherradi, S.E., Santoro, M., Ramammoorthy, V., Menegaz, B.A., Bartholomeusz, G., Iles, L.R., Amin, H.M., Livingston, J.A., Mikos, A.G., and Ludwig, J.A. (2014). 3D tissue-engineered model of Ewing's sarcoma. Adv. Drug Deliv. Rev. *79–80*, 155–171. https://doi.org/10.1016/j.addr.2014.07.012.
6. Cantor, J.R. (2019). The Rise of Physiologic Media. Trends Cell Biol. *29*, 854–861. https://doi.org/10.1016/j.tcb.2019.08.009.
7. Fleuren, E.D.G., Versleijen-Jonkers, Y.M.H., Boerman, O.C., and van der Graaf, W.T.A. (2014). Targeting receptor tyrosine kinases in osteosarcoma and Ewing sarcoma: current hurdles and future perspectives. Biochim. Biophys. Acta *1845*, 266–276. https://doi.org/10.1016/j.bbcan.2014.02.005.
8. Marturano-Kruik, A., Villasante, A., Yaeger, K., Ambati, S.R., Chramiec, A., Raimondi, M.T., and Vunjak-Novakovic, G. (2018). Biomechanical regulation of drug sensitivity in an engineered model of human tumor. Biomaterials *150*, 150–161. https://doi.org/10.1016/j.biomaterials.2017.10.020.
9. Sole, A., Grossetête, S., Heintzé, M., Babin, L., Zaïdi, S., Revy, P., Renouf, B., De Cian, A., Giovannangeli, C., Pierre-Eugène, C., et al. (2021). Unraveling Ewing Sarcoma Tumorigenesis Originating from Patient-Derived Mesenchymal Stem Cells. Cancer Res. *81*, 4994–5006. https://doi.org/10.1158/0008-5472.CAN-20-3837.
10. Cidre-Aranaz, F., and Ohmura, S. (2021). Tumor Growth Analysis of Ewing Sarcoma Cell Lines Using Subcutaneous Xenografts in Mice. Methods Mol. Biol. *2226*, 191–199.
11. Surdez, D., Landuzzi, L., Scotlandi, K., and Manara, M.C. (2021). Ewing Sarcoma PDX Models. Methods Mol. Biol. *2226*, 223–242. https://doi.org/10.1007/978-1-0716-1020-6_18.
12. Ramachandran, B., Rajkumar, T., and Gopisetty, G. (2021). Challenges in modeling EWS-FLI1-driven transgenic mouse model for Ewing sarcoma. Am. J. Transl. Res. *13*, 12181–12194.
13. Koledova, Z. (2017). 3D Cell Culture: An Introduction. Methods Mol. Biol. *1612*, 1–11. https://doi.org/10.1007/978-1-4939-7021-6_1.
14. Cantor, J.R., Abu-Remaileh, M., Kanarek, N., Freinkman, E., Gao, X., Louissaint, A., Jr., Lewis, C.A., and Sabatini, D.M. (2017). Physiologic Medium Rewires Cellular Metabolism and Reveals Uric Acid as an Endogenous Inhibitor of UMP Synthase. Cell *169*, 258–272. https://doi.org/10.1016/j.cell.2017.03.023.
15. Vande Voorde, J., Ackermann, T., Pfetzer, N., Sumpton, D., Mackay, G., Kalna, G., Nixon, C., Blyth, K., Gottlieb, E., and Tardito, S. (2019). Improving the metabolic fidelity of cancer models with a physiological cell culture medium. Sci. Adv. *5*, eaau7314. https://doi.org/10.1126/sciadv.aau7314.

16. Ackermann, T., and Tardito, S. (2019). Cell Culture Medium Formulation and Its Implications in Cancer Metabolism. Trends Cancer *5*, 329–332. https://doi.org/10.1016/j.trecan.2019.05.004.

17. Leney-Greene, M.A., Boddapati, A.K., Su, H.C., Cantor, J.R., and Lenardo, M.J. (2020). Human Plasma-like Medium Improves T Lymphocyte Activation. iScience *23*, 100759. https://doi.org/10.1016/j.isci.2019.100759.

18. Flickinger, K.M., Wilson, K.M., Rossiter, N.J., Hunger, A.L., Vishwasrao, P.V., Lee, T.D., Mellado Fritz, C.A., Richards, R.M., Hall, M.D., and Cantor, J.R. (2024). Conditional lethality profiling reveals anticancer mechanisms of action and drug-nutrient interactions. Sci. Adv. *10*, eadq3591. https://doi.org/10.1126/sciadv.adq3591.

19. van der Valk, J. (2022). Fetal bovine serum-a cell culture dilemma. Science *375*, 143–144. https://doi.org/10.1126/science.abm1317.

20. Gstraunthaler, G. (2003). Alternatives to the use of fetal bovine serum: serum-free cell culture. ALTEX *20*, 275–281.

21. van Gorsel, M., Elia, I., and Fendt, S.M. (2019). 13C Tracer Analysis and Metabolomics in 3D Cultured Cancer Cells. Methods Mol. Biol. *1862*, 53–66. https://doi.org/10.1007/978-1-4939-8769-6_4.

22. Orth, M.F., Surdez, D., Faehling, T., Ehlers, A.C., Marchetto, A., Grossetête, S., Volckmann, R., Zwijnenburg, D.A., Gerke, J.S., Zaidi, S., et al. (2022). Systematic multi-omics cell line profiling uncovers principles of Ewing sarcoma fusion oncogene-mediated gene regulation. Cell Rep. *41*, 111761. https://doi.org/10.1016/j.celrep.2022.111761.

23. Brohl, A.S., Solomon, D.A., Chang, W., Wang, J., Song, Y., Sindiri, S., Patidar, R., Hurd, L., Chen, L., Shern, J.F., et al. (2014). The genomic landscape of the Ewing Sarcoma family of tumors reveals recurrent STAG2 mutation. PLoS Genet. *10*, e1004475. https://doi.org/10.1371/journal.pgen.1004475.

24. Tirode, F., Surdez, D., Ma, X., Parker, M., Le Deley, M.C., Bahrami, A., Zhang, Z., Lapouble, E., Grossetête-Lalami, S., Rusch, M., et al. (2014). Genomic landscape of Ewing sarcoma defines an aggressive subtype with co-association of STAG2 and TP53 mutations. Cancer Discov. *4*, 1342–1353. https://doi.org/10.1158/2159-8290.Cd-14-0622.

25. Torres-Quesada, O., Doerrier, C., Strich, S., Gnaiger, E., and Stefan, E. (2022). Physiological Cell Culture Media Tune Mitochondrial Bioenergetics and Drug Sensitivity in Cancer Cell Models. Cancers *14*, 3917. https://doi.org/10.3390/cancers14163917.

26. Riffle, S., Pandey, R.N., Albert, M., and Hegde, R.S. (2017). Linking hypoxia, DNA damage and proliferation in multicellular tumor spheroids. BMC Cancer *17*, 338. https://doi.org/10.1186/s12885-017-3319-0.

27. Redini, F., and Heymann, D. (2015). Bone Tumor Environment as a Potential Therapeutic Target in Ewing Sarcoma. Front. Oncol. *5*, 279. https://doi.org/10.3389/fonc.2015.00279.

28. Baldauf, M.C., Gerke, J.S., Kirschner, A., Blaeschke, F., Effenberger, M., Schober, K., Rubio, R.A., Kanaseki, T., Kiran, M.M., Dallmayer, M., et al. (2018). Systematic identification of cancer-specific MHC-binding peptides with RAVEN. OncoImmunology *7*, e1481558. https://doi.org/10.1080/2162402X.2018.1481558.

29. Postel-Vinay, S., Véron, A.S., Tirode, F., Pierron, G., Reynaud, S., Kovar, H., Oberlin, O., Lapouble, E., Ballet, S., Lucchesi, C., et al. (2012). Common variants near TARDBP and EGR2 are associated with susceptibility to Ewing sarcoma. Nat. Genet. *44*, 323–327. https://doi.org/10.1038/ng.1085.

30. Kinsey, M., Smith, R., and Lessnick, S.L. (2006). NR0B1 is required for the oncogenic phenotype mediated by EWS/FLI in Ewing's sarcoma. Mol. Cancer Res. *4*, 851–859. https://doi.org/10.1158/1541-7786.MCR-06-0090.

31. Franzetti, G.A., Laud-Duval, K., van der Ent, W., Brisac, A., Irondelle, M., Aubert, S., Dirksen, U., Bouvier, C., de Pinieux, G., Snaar-Jagalska, E., et al. (2017). Cell-to-cell heterogeneity of EWSR1-FLI1 activity determines proliferation/migration choices in Ewing sarcoma cells. Oncogene *36*, 3505–3514. https://doi.org/10.1038/onc.2016.498.

32. Aynaud, M.M., Mirabeau, O., Gruel, N., Grossetête, S., Boeva, V., Durand, S., Surdez, D., Saulnier, O., Zaïdi, S., Gribkova, S., et al. (2020). Transcriptional Programs Define Intratumoral Heterogeneity of Ewing Sarcoma at Single-Cell Resolution. Cell Rep. *30*, 1767–1779.e6. https://doi.org/10.1016/j.celrep.2020.01.049.

33. Tardito, S., and MacKay, C. (2023). Rethinking our approach to cancer metabolism to deliver patient benefit. Br. J. Cancer *129*, 406–415. https://doi.org/10.1038/s41416-023-02324-9.

34. de Jonge, H.J.M., Fehrmann, R.S.N., de Bont, E.S.J.M., Hofstra, R.M.W., Gerbens, F., Kamps, W.A., de Vries, E.G.E., van der Zee, A.G.J., te Meerman, G.J., and ter Elst, A. (2007). Evidence based selection of housekeeping genes. PLoS One *2*, e898. https://doi.org/10.1371/journal.pone.0000898.

35. Joshi, C.J., Ke, W., Drangowska-Way, A., O'Rourke, E.J., and Lewis, N.E. (2022). What are housekeeping genes? PLoS Comput. Biol. *18*, e1010295. https://doi.org/10.1371/journal.pcbi.1010295.

36. Ceranski, A.K., Carreño-Gonzalez, M.J., Ehlers, A.C., Colombo, M.V., Cidre-Aranaz, F., and Grünewald, T.G.P. (2023). Hypoxia and HIFs in Ewing sarcoma: new perspectives on a multi-facetted relationship. Mol. Cancer *22*, 49. https://doi.org/10.1186/s12943-023-01750-w.

37. Rossiter, N.J., Huggler, K.S., Adelmann, C.H., Keys, H.R., Soens, R.W., Sabatini, D.M., and Cantor, J.R. (2021). CRISPR screens in physiologic medium reveal conditionally essential genes in human cells. Cell Metabol. *33*, 1248–1263. https://doi.org/10.1016/j.cmet.2021.02.005.

38. Buttgereit, F., and Brand, M.D. (1995). A hierarchy of ATP-consuming processes in mammalian cells. Biochem. J. *312*, 163–167. https://doi.org/10.1042/bj3120163.

39. Lindqvist, L.M., Tandoc, K., Topisirovic, I., and Furic, L. (2018). Cross-talk between protein synthesis, energy metabolism and autophagy in cancer. Curr. Opin. Genet. Dev. *48*, 104–111. https://doi.org/10.1016/j.gde.2017.11.003.

40. Warren, A., Chen, Y., Jones, A., Shibue, T., Hahn, W.C., Boehm, J.S., Vazquez, F., Tsherniak, A., and McFarland, J.M. (2021). Global computational alignment of tumor and cell line transcriptional profiles. Nat. Commun. *12*, 22. https://doi.org/10.1038/s41467-020-20294-x.

41. Subramanian, A., Tamayo, P., Mootha, V.K., Mukherjee, S., Ebert, B.L., Gillette, M.A., Paulovich, A., Pomeroy, S.L., Golub, T.R., Lander, E.S., and Mesirov, J.P. (2005). Gene set enrichment analysis: a knowledge-based approach for interpreting genome-wide expression profiles. Proc. Natl. Acad. Sci. USA *102*, 15545–15550. https://doi.org/10.1073/pnas.0506580102.

42. Langfelder, P., and Horvath, S. (2008). WGCNA: an R package for weighted correlation network analysis. BMC Bioinf. *9*, 559. https://doi.org/10.1186/1471-2105-9-559.

43. Hulsen, T. (2022). DeepVenn – a web application for the creation of area-proportional Venn diagrams using the deep learning framework Tensorflow.js. arXiv. https://doi.org/10.48550/arXiv.2210.04597.

44. Gautier, L., Cope, L., Bolstad, B.M., and Irizarry, R.A. (2004). affy–analysis of Affymetrix GeneChip data at the probe level. Bioinformatics *20*, 307–315. https://doi.org/10.1093/bioinformatics/btg405.

45. Irizarry, R.A., Hobbs, B., Collin, F., Beazer-Barclay, Y.D., Antonellis, K.J., Scherf, U., and Speed, T.P. (2003). Exploration, normalization, and summaries of high density oligonucleotide array probe level data. Biostatistics *4*, 249–264. https://doi.org/10.1093/biostatistics/4.2.249.

46. Dai, M., Wang, P., Boyd, A.D., Kostov, G., Athey, B., Jones, E.G., Bunney, W.E., Myers, R.M., Speed, T.P., Akil, H., et al. (2005). Evolving gene/transcript definitions significantly alter the interpretation of GeneChip data. Nucleic Acids Res. *33*, e175. https://doi.org/10.1093/nar/gni179.

47. Hänzelmann, S., Castelo, R., and Guinney, J. (2013). GSVA: gene set variation analysis for microarray and RNA-seq data. BMC Bioinf. *14*, 7. https://doi.org/10.1186/1471-2105-14-7.

48. Johnson, W.E., Li, C., and Rabinovic, A. (2007). Adjusting batch effects in microarray expression data using empirical Bayes methods. Biostatistics *8*, 118–127. https://doi.org/10.1093/biostatistics/kxj037.

49. Gu, Z., Eils, R., and Schlesner, M. (2016). Complex heatmaps reveal patterns and correlations in multidimensional genomic data. Bioinformatics *32*, 2847–2849. https://doi.org/10.1093/bioinformatics/btw313.

50. Ritchie, M.E., Phipson, B., Wu, D., Hu, Y., Law, C.W., Shi, W., and Smyth, G.K. (2015). limma powers differential expression analyses for RNA-sequencing and microarray studies. Nucleic Acids Res. *43*, e47. https://doi.org/10.1093/nar/gkv007.

51. Korotkevich, G., Sukhov, V., Budin, N., Shpak, B., Artyomov, M.N., and Sergushichev, A. (2021). Fast gene set enrichment analysis. bioRxiv. https://doi.org/10.1101/060012.

52. Wu, T., Hu, E., Xu, S., Chen, M., Guo, P., Dai, Z., Feng, T., Zhou, L., Tang, W., Zhan, L., et al. (2021). clusterProfiler 4.0: A universal enrichment tool for interpreting omics data. Innovation *2*, 100141. https://doi.org/10.1016/j.xinn.2021.100141.

53. Mi, H., Muruganujan, A., Ebert, D., Huang, X., and Thomas, P.D. (2019). PANTHER version 14: more genomes, a new PANTHER GO-slim and improvements in enrichment analysis tools. Nucleic Acids Res. *47*, D419–D426. https://doi.org/10.1093/nar/gky1038.

54. Musa, J., and Cidre-Aranaz, F. (2021). Drug Screening by Resazurin Colorimetry in Ewing Sarcoma. Methods Mol. Biol. *2226*, 159–166. https://doi.org/10.1007/978-1-0716-1020-6_12.

55. Funk, C.M., and Musa, J. (2021). Proliferation Assessment by Trypan Blue Exclusion in Ewing Sarcoma. Methods Mol. Biol. *2226*, 151–158.

56. Schneider, C.A., Rasband, W.S., and Eliceiri, K.W. (2012). NIH Image to ImageJ: 25 years of image analysis. Nat. Methods *9*, 671–675. https://doi.org/10.1038/nmeth.2089.

57. Marchetto, A., Ohmura, S., Orth, M.F., Knott, M.M.L., Colombo, M.V., Arrigoni, C., Bardinet, V., Saucier, D., Wehweck, F.S., Li, J., et al. (2020). Oncogenic hijacking of a developmental transcription factor evokes vulnerability toward oxidative stress in Ewing sarcoma. Nat. Commun. *11*, 2423. https://doi.org/10.1038/s41467-020-16244-2.

58. Waszak, S.M., Robinson, G.W., Gudenas, B.L., Smith, K.S., Forget, A., Kojic, M., Garcia-Lopez, J., Hadley, J., Hamilton, K.V., Indersie, E., et al. (2020). Germline Elongator mutations in Sonic Hedgehog medulloblastoma. Nature *580*, 396–401. https://doi.org/10.1038/s41586-020-2164-5.

STAR★METHODS

KEY RESOURCES TABLE

REAGENT or RESOURCE	SOURCE	IDENTIFIER
Antibodies		
Rabbit monoclonal anti-FLI1	Abcam, Cambridge, UK	Cat#ab133485; RRID:AB_2722650
Rabbit monoclonal anti-ERG	Abcam, Cambridge, UK	Cat#ab92513; RRID:AB_2630401
Rabbit monoclonal anti-GAPDH	Cell Signaling Technology, Danvers, MA, USA	Cat#2118, RRID:AB_561053
Polyclonal anti-rabbit IgG-HRP raised in goat	Thermo Fisher, Waltham, MA, USA	Cat#31460
Chemicals, peptides, and recombinant proteins		
Roswell Park Memorial Institute (RPMI) medium	Thermo Fisher, Waltham, MA, USA	Cat#11875093
Human Plasma-Like Medium (HPLM)	Thermo Fisher, Waltham, MA, USA	Cat#A4899101
(+)-Sodium L-ascorbate	Merck, Darmstadt, Germany	Cat#A4034
L-Homocysteine	Merck, Darmstadt, Germany	Cat#69453
L-Pyroglutamic acid	Merck, Darmstadt, Germany	Cat#P5960
2-Hydroxybutyric acid sodium salt	Merck, Darmstadt, Germany	Cat#220116
L-Carnosine	Merck, Darmstadt, Germany	Cat#C9625
Sodium (*S*)-β-hydroxyisobutyrate	Merck, Darmstadt, Germany	Cat#16842
Methyl acetoacetate	Merck, Darmstadt, Germany	Cat#537365
Uracil	Merck, Darmstadt, Germany	Cat#U1128
Iron(III) nitrate nonahydrate	Merck, Darmstadt, Germany	Cat#F8508
Zinc sulfate heptahydrate	Merck, Darmstadt, Germany	Cat#Z0251
Copper(II) sulfate pentahydrate	Merck, Darmstadt, Germany	Cat#C8027
Sodium selenite	Merck, Darmstadt, Germany	Cat#S5261
Manganese(II) chloride tetrahydrate	Merck, Darmstadt, Germany	Cat#M5005
Agar Agar high gel-strength powder	SERVA Electrophoresis GmbH, Heidelberg, Germany	Cat#11396.03
Doxycycline (dox)	Merck, Darmstadt, Germany	Cat#324385
Penicillin-Streptomycin	Merck, Darmstadt, Germany	Cat#P0781
Collagen coating solution	Hölzel Diagnostika Handels GmbH, Köln, Germany	Cat#PMC-SCO
DPBS, no calcium, no magnesium	Thermo Fisher, Waltham, MA, USA	Cat#14190144
Fetal Calf Serum	Merck, Darmstadt, Germany	Cat#F7524
Puromycin (10 mg/mL solution)	InvivoGen, San Diego, CA, USA	Cat#ant-pr-1
Trypsin/EDTA	Pan Biotech, Aidenbach, Germany	Cat#P10-024100
Critical commercial assays		
High-Capacity cDNA Reverse Transcription Kit	Thermo Fisher, Waltham, MA, USA	Cat#4368814
NucleoSpin RNA kit	Macherey-Nagel, Düren, Germany	Cat#740955
SYBR SELECT Master Mix	Thermo Fisher, Waltham, MA, USA	Cat#4472908
NucleoSpin Tissue genomic DNA prep kit	Macherey-Nagel, Düren, Germany	Cat#740952
Deposited data		
Transcriptome data (DNA microarrays) from 4 EwS cell lines in refined culture condition with increased physiological relevance in EWSR1-ETS-high and -low condition; raw and processed data	This paper	GSE270118

(*Continued on next page*)

Continued

REAGENT or RESOURCE	SOURCE	IDENTIFIER
Transcriptome data (DNA microarrays) from 4 EwS cell lines cultured in standard condition in EWSR1-ETS-high and -low condition; raw and processed data	ESCLA, Orth et al.[22]	GSE176190
Transcriptome data (DNA microarrays) from patient tumors in multiple cancer entities including 50 EwS patient tumors; raw and processed data	Baldauf et al.[28]	https://github.com/JSGerke/RAVENsoftware/releases/microarrayRNA_pediatric-sarcoma.zip; https://doi.org/10.1080/2162402X.2018.1481558
Transcriptome data (DNA microarrays) from EwS primary patient tumors; raw and processed data	Postel-Vinay et al.[29]	GSE34620
Experimental models: Cell lines		
A-673/TR/shEF1	ESCLA, Orth et al.,[22] lab of T.G.P. Grünewald	For WT cell line: RRID: CVCL_0080
MHH-ES-1/TR/shEF1	ESCLA, Orth et al.,[22] lab of T.G.P. Grünewald	For WT cell line: RRID: CVCL_1411
SK-N-MC/TR/shEF1	ESCLA, Orth et al.,[22] lab of T.G.P. Grünewald	For WT cell line: RRID: CVCL_0530
TC-71/TR/shEF1	ESCLA, Orth et al.,[22] lab of T.G.P. Grünewald	For WT cell line: RRID: CVCL_2213
TC-106/TR/shEERG	ESCLA, Orth et al.,[22] lab of T.G.P. Grünewald	For WT cell line: RRID: CVCL_F531
Oligonucleotides		
Primers, for sequence details see STAR Methods section	eurofins Genomics, Ebersberg, Germany	N/A
Software and algorithms		
Transcriptome Analysis Console (4.0)	Thermo Fisher, Waltham, MA, USA	https://www.thermofisher.com/de/en/home/life-science/microarray-analysis/microarray-analysis-instruments-software-services/microarray-analysis-software/affymetrix-transcriptome-analysis-console-software.html
Gene Set Enrichment Analysis	Subramanian et al.[41]	https://www.gsea-msigdb.org/gsea/index.jsp
Weighted Correlation Network Analysis R package	Langfelder and Horvath[42]	https://bmcbioinformatics.biomedcentral.com/articles/10.1186/1471-2105-9-559
GraphPad PRISM (version 10)	GraphPad Software Inc., CA, USA	https://www.graphpad.com/scientific-software/prism/
DeepVenn web application	Hulsen[43]	https://arxiv.org/abs/2210.04597
Affy package version 1.78.2	Gautier et al.[44]	https://doi.org/10.18129/B9.bioc.affy
Robust Multi-chip Average (RMA) algorithm	Irizarry et al.[45]	https://rdrr.io/bioc/xps/man/rma.html
Custom Brainarray Chip Description Files	Dai et al.[46]	http://brainarray.mbni.med.umich.edu/Brainarray/Database/CustomCDF/genomic_curated_CDF.asp
GSVA package version 1.48.3	Hänzelmann et al.[47]	https://doi.org/10.18129/B9.bioc.GSVA
ComBat function from the sva package version 3.48.0	Johnson et al.[48]	https://doi.org/10.18129/B9.bioc.sva
ComplexHeatmap package version 2.16.0	Gu et al.[49]	https://doi.org/10.18129/B9.bioc.ComplexHeatmap
limma version 3.58.1	Ritchie et al.[50]	https://doi.org/10.18129/B9.bioc.limma
fGSEA version 1.28.0	Korotkevich et al.[51]	https://doi.org/10.18129/B9.bioc.fgsea
clusterProfiler version 4.10.1	Wu et al.[52]	https://doi.org/10.18129/B9.bioc.clusterProfiler
PANTHER	Mi et al.[53]	https://pantherdb.org/

CellPress
OPEN ACCESS

EXPERIMENTAL MODEL AND STUDY PARTICIPANT DETAILS

Provenance of cell lines

The EwS cell line A-673 (RRID CVCL_0080) was obtained from American Type Culture Collection (ATCC, Manassas, USA), and MHH-ES-1 (CVCL_1411), SK-N-MC (CVCL_0530), and TC-71 (CVCL_2213) were obtained from the German Collection of Microorganisms and Cell cultures GmbH (DSMZ, Braunschweig, Germany). The EwS cell line TC-106 (CVCL_F531) was obtained from the Children's Oncology Group (COG). Cell identity was regularly confirmed by single-nucleotide polymorphism (SNP) and/or short tandem repeat (STR) profiling. Genetic sex was ascertained from WGS data and corresponds to the genetic sex reported previously[22] for all cell lines from this study.

Culture conditions for cell lines

For standard culture conditions, all cell lines were cultured in RPMI 1640 medium with stable glutamine (Biochrom, Germany), supplemented with 10% FCS tested to be doxycycline (dox)-free (Sigma-Aldrich, Germany), and penicillin (100 U/mL) and streptomycin (100 μg/mL; Merck, Germany) in tissue culture flasks and plates (Sarstedt, Germany). For TC-106, culture dishes were coated with collagen coating solution (Sigma-Aldrich) and either directly used or stored at 4°C for max two weeks.

For refined culture conditions, all cell lines were cultured in HPLMax (protocol for fabrication see below; details of the composition are given in Table S1), supplemented with 7% FCS tested to be dox-free (Sigma-Aldrich, Germany), and penicillin (100 U/mL) and streptomycin (100 μg/mL; Merck, Germany) in tissue culture flasks and plates (Sarstedt, Germany) coated with 2 mL of 1.5% high gel-strength agar (Serva) to generate ultra-low attachment conditions for spheroid formation.[21] Coated flasks were either directly used or stored at 4°C for max 2 weeks.

In both culture conditions, cells were incubated at 37°C and 5% CO_2 in a fully humidified environment. Cells were subcultured in ratios 1:2 to 1:8 after detachment with trypsin/EDTA (Biochrom). Cultures were routinely tested for and found to be free of Mycoplasma contamination by nested PCR.

Spheroid seeding

For seeding of cells for spheroid formation, previously 2D grown cells in HPLMax supplemented with 7% FCS were used. Respective cell numbers of A-673/TR/shEF1 (1.2×10^6 cells), SK-N-MC/TR/shEF (1×10^6 cells), MHH-ES-1/TR/shEF1 (1.8×10^6 cells), TC-71/TR/shEF1 (1×10^6 cells) and TC-106/TR/shEERG (1.2×10^6 cells) were seeded in triplicates per condition (dox+/−) in five mL of HPLMax, 7% FCS, in agar-coated T-25 flasks (see description for refined culture conditions above). Cells were cultured for sphere formation for four days.

METHOD DETAILS

Fabrication HPLMax

For the refined cell culture conditions of EwS cell lines, we used a combination of two media which reflect metabolite concentrations of human plasma, namely HPLM and Plasmax.[14,15] Our combination, called HPLMax, is based on the readily available HPLM[14] medium to which we added manually 13 additional metabolites, that are only included in the Plasmax recipe.[15] An overview on the compositions of HPLM and Plasmax[14,15] is given in Table S1. For the 13 additional metabolites, single stock solutions were prepared according to Table S1 and stored at −20°C. For preparation of HPLMax, the 13 Plasmax metabolite single stock solutions were combined, filter sterilized and added to HPLM[14] as according to Table S1.

Cell lines with *EWSR1::ETS*-knockdown

We used 5 previously generated EwS cell lines with inducible knockdown of the fusion oncogene.[22] Briefly, EwS cell lines were lentivirally transduced with an pLKO-Tet-On all-in-one vector containing a dox-inducible shRNA against the respective *EWSR1::ETS* fusion or against its constituting *ETS* parts (*FLI1* or *ERG*).[22] Efficient gene silencing was confirmed by qRT-PCR and led to a remaining fusion gene expression of ∼20% and previously performed western blot confirmed knockdown of the respective EWSR1:ETS fusions at the protein level.[22] These established cell lines were regularly selected with 1 mg/mL puromycin (Invivogen). The shRNA mediated knockdown of the respective *EWSR1::ETS* fusion oncogenes was induced by addition of 1 μg/mL dox (Merck, Germany) to the cell culture medium. Dox was refreshed every 48 h. Afterward, expression of the given *EWSR1::ETS* fusion and knockdown efficiency was assessed by qRT-PCR.

Proliferation assays

Proliferation of EwS cells was assessed by resazurin colorimetry[54] or trypan blue exclusion.[55] In brief, a previously described drug screening by resazurin colorimetry in EwS[54] was adapted to test cell growth in different FCS concentrations. A-673/TR/shEF1 (6×10^3 cells), SK-N-MC/TR/shEF1 (5×10^3 cells), MHH-ES-1/TR/shEF1 (5×10^3 cells), TC-71/TR/shEF1 (4×10^3 cells) and TC-106/TR/shEERG (5×10^3 cells) were seeded in 96-well plates (Sarstedt, Germany) in 1–10% FCS supplementation in RPMI, and readout was

performed after 96 h incubation according to the previously published protocol.[54] Trypan-Blue exclusion was performed as described.[55] In brief, 3–20 × 10 cells were seeded in 6-well plates in 10% or 7% FCS supplemented media and viable and dead cells were manually counted after 96 h.

Spheroid histology

Spheroids were seeded as described above. After 96 h of spheroid formation and additional 96 h of treatment with dox+/−, spheroids were harvested on day 9 after seeding. Spheroids were collected, incubated in 4% buffered paraformaldehyde (PFA) for 15 min at RT, then embedded into a cryomold (Sakura Finetek, USA) containing 3% agar. Once solidified, the agar pad was transferred into a histology cassette. The cassette was put in 4% buffered PFA overnight and transferred into a 50% alcohol solution the next day. Then, water extraction and embedding in paraffin was conducted by the DKFZ Light Microscopy Core Facility. Paraffin blocks were cut into slices of 3 μm, transferred onto microscope slides and stained with hematoxylin and eosin (H&E). For comparison, H&E stains of archival subcutaneous xenografts of wildtype TC-71 cells were used.[10]

RNA extraction and qRT-PCR

For RNA extraction, the NucleoSpin RNA kit from Macherey-Nagel (Duren, Germany) was used following the manufacturer's protocol. Isolated RNA (1 mg, quantified with NanoDrop) was reverse transcribed applying the High-Capacity cDNA Reverse Transcription Kit (Thermo Fisher) following the manufacturer's protocol. qRT-PCR reactions contained 9 μL 1:10 diluted cDNA, 10 μL SYBR Select Mastermix (Thermo Fisher) and 1 μL mix of forward and reverse primer (final concentration 0.5 mM) in a final volume of 20 μL. Reactions were carried out in duplicates or triplicates with a CFX Connect Real-Time PCR Detection System (Bio-Rad, Munich, Germany). Relative expression was calculated by the ΔΔCt method and normalized against either *ribosomal protein lateral stalk subunit P0* (*RPLP0*), *RNA component of 7SK nuclear ribonucleoprotein* (*RN7SK*), or *glyceraldehyde-3-phosphate dehydrogenase* (*GAPDH*). Stable expression of *RPLP0* in EwS cell culture conditions with RPMI medium has been shown in previously[22] and our data suggested that *RN7SK* and *GAPDH* are among the suitable HKGs for comparison of gene expression levels in EwS cell lines in the refined culture conditions. The following primer sequences (eurofins Genomics, Ebersberg, Germany) were used: *RPLP0* forward: 5′- GAAACTCTGCATTCTC GCTTC -3'; *RPLP0* reverse: 5′- GGTGTAATCCGTCTCCACAG -3'; *EWSR1::FLI1* forward: 5′- GCCAAGCTCCAAGTCAATATAGC -3'; *EWSR1::FLI1* reverse: 5′- GAGGCCAGAATTCATGTTATTGC -3'; *EWSR1::ERG* forward: 5′- TCCAAGTCAATATAGCCAACAGAG -3'; *EWSR1::ERG* reverse: 5′- CTGTGGAAGGAGATGGTTGAG -3'; *RN7SK* forward: 5′- ATTGATCGCCACCCTTGAT -3'; *RN7SK* reverse: 5′- CTCTATCGGGGATGGTCGT –3'; *GAPDH* forward: 5′- CTTCAACAGCGACACCCACT -3'; *GAPDH* reverse: 5′- GTGGTCCA GGGGTCTTACTC-3'.

Western blot

For lysing, pellets were put in 50 μL RIPA buffer (Serva electrophoresis) with protease inhibitor (Sigma-Aldrich, Germany). Protein concentration was measured by BCA assay (Thermo Fisher Scientific). Before loading the samples on the western blot gel, 20 μg of protein were denaturized at 95°C for 5 min. Then, with a 10% acrylamide gel (Bio-Rad, Munich, Germany) the samples were separated and blotted onto a PVDF membrane (Bio-Rad, Munich, Germany) that was pre-activated in 100% methanol, using a TurboTransfer system (Bio-Rad, Munich, Germany). The membrane was blocked for 1 h at RT with 5% non-fat dairy milk in TBS-T. Incubation with the first antibody was done overnight at 4°C in the following dilutions: AntiFLI1 1:1,000, 5% milk, AntiERG 1:1,000, 5% milk, AntiGAPDH 1:2,000, 5% milk. The next day, washing was done with TBS-T followed by incubation with the corresponding second antibody (coupled with horseradish peroxidase) for 1 h at RT at the following concentrations: AntiFLI1 and AntiERG 1:2,000, AntiGAPDH 1:5,000. After washing with TBST-T, bands were detected by electrochemiluminescence with Chemiluminescent HRP Substrate (Biozym, Germany). Quantification of the bands was done by densitometry using ImageJ.[56] The following antibodies were used: monoclonal anti-FLI1 raised in rabbit (1:1,000, EPR4646, ab133485, Abcam), monoclonal anti-ERG raised in rabbit (1:1,000, EPR3864, ab92513, Abcam), monoclonal anti-GAPDH raised in rabbit (1:2,000, GAPDH 14C10, #2118, Cell Signaling), and polyclonal anti-rabbit IgG-HRP raised in goat (1:2,000, cat # 31460, Thermo Fisher Scientific).

Transcriptome analyses

To study the EWSR1::ETS activity in refined culture conditions in EwS cells, microarray analysis was performed. Four selected EwS cell lines were seeded in triplicates for each condition (dox+/−) as described above for spheroid seeding and cultured for 8 days, with dox refreshed every 48 h. Spheroids were collected on day 9, pelleted, then resuspended in lysis buffer from NucleoSpin RNA kit (Macherey-Nagel, Germany). Further RNA extraction followed the manufacturer's protocol. RNA (1 mg, quantified with NanoDrop) was checked for quality with a tape station using the RNA ScreenTape Analysis kit (Agilent) according to manufacturer's protocol. RNA integrity number was $\geq$8.5 for all samples. Knockdown efficiency was assessed as described above and remaining expression of *EWSR1::ETS* was confirmed to be <30% of untreated samples. Samples were hybridized to Human Affymetrix Clariom D microarrays. The retrieved raw expression data were subjected to joint processing and analysis, including background correction, normalization, and gene-level summarization, with the previously generated data from standard culture condition.[22] Of note, experimental procedures of dox treatment, RNA extraction, and RNA concentration for microarray profiling were identical in both experiments conducted under refined and standard culture conditions to minimize impact of potential batch effects. Data were quantile normalized

and summarized with Transcriptome Analysis Console (v4.0; Thermo Fisher Scientific) using the SST-RMA algorithm.[57] The data were annotated with the Affymetrix library for Clariom D array (version 2, homo sapiens) at gene level. This resulted in a list of 21,324 unique annotated genes. Exploratory data analysis was conducted with PCA to identify captured variation in the transcriptomic data. For identification of DEGs for each comparison of interest with significant and consistent fold changes (FCs) across all cell lines, normalized log2 gene expression values were subjected to DEG analysis with limma (v 3.58.1).[50] DEGs were defined as having adjusted $p < 0.05$ and arbitrarily |log2 FC| >1.5.

Comparison and distance calculations of EwS patient tumor and in vitro gene expression profiles

The above-described preprocessed and normalized microarray gene expression data from the two different *in vitro* conditions ($n = 48$) and patient tumor samples ($n = 2,678$) were integrated using ComBat batch correction[48] from the sva package to remove systematic batch effects while preserving biological variation. The tumor samples, representing multiple cancer entities including EwS, were downloaded as provided by Baldauf et al.[28] The merged dataset contained 16,925 common genes. For EwS-specific analyses, we subset samples for included EwS tumors ($n = 50$) and EwS cell line samples, retaining only samples without induced EWSR1:FLI1 fusion knockdown (no dox; HPLMax_high and RPMI_high, $n = 12$ each, $n = 74$ total). Principal Component Analysis (PCA) was performed on the scaled expression matrix.

To further assess the similarity between culture conditions and tumor samples, we calculated pairwise distances between all samples using Pearson correlation-based distances. One-sided Wilcoxon rank-sum tests were used to assess whether 'refined *in vitro* – tumor' distances were significantly smaller than 'standard *in vitro* – tumor' distances.

Single sample gene-set enrichment analyses (ssGSEA)

The above-described preprocessed and normalized microarray gene expression data from the EwS cell lines in two different culture conditions without dox treatment ($n = 24$) were taken as input files and combined with a publicly available and well-curated gene expression dataset of EwS patient tumors ($n = 117$; GEO accession code GSE34620)[29] generated on GeneChip Human Genome U133 Plus 2.0 Array microarrays (Applied Biosystems, Waltham, MA, USA). To generate input files from the EwS patient tumors, microarray *.CEL files were preprocessed and normalized simultaneously in R version 4.3.0 using the affy package version 1.78.2.[44] For this, the Robust Multi-chip Average (RMA) algorithm, including background adjustment, quantile normalization and summarization was applied.[45] For RMA normalization custom brainarray Chip Description Files (CDF; ENTREZG, v25) were used, yielding one optimized probe set per gene.[46] With the input files, ssGSEA was performed using the GSVA package in R version 1.48.3[50]. The analysis was restricted to genes covered on both the GeneChip Human Genome U133 Plus 2.0 Array microarrays and Affymetrix Clariom D microarray. Enrichment scores were calculated for a previously described EWSR1:ETS signature[22] as well as gene sets from the Molecular Signatures Database (MSigDB, h.all.v7.0.symbols.gmt, c2.cgp.v7.0.symbols.gmt, c5.all.v7.0.symbols.gmt) and the 'top1,000byexpression' gene set, which consisted of the 1,000 genes with the highest mean expression across all EwS patient tumors analyzed. The resulting normalized enrichment scores (NES) were used for downstream statistical analyses and visualization. Heatmaps were annotated in R with ComplexHeatmap package version 2.16.0.[49]

Pathway enrichment analysis

To identify enriched gene sets, all genes were ranked by their mean log2 FC for each comparison of interest and used as input for pre-ranked GSEA.[41] The analysis was conducted using fGSEA (v 1.28.0)[51] with gene sets from the Molecular Signatures Database (MSigDB, h.all.v7.0.symbols.gmt, c2.cgp.v7.0.symbols.gmt, c5.all.v7.0.symbols.gmt). Enrichment plots for individual gene signatures were generated using the enrichplot package (v 1.22.0), clusterProfiler (v 4.10.1).[52] Enriched gene ontology (GO) terms, defined as adjusted $p < 0.05$ and |NES|>2 (10,000 permutations), were employed for network construction though the use of Weighted Correlation Network Analysis (WGCNA, v 1.72–5).[42] In a first step, a binary matrix of GO terms and genes (in which 1 signifies that the gene is present in the GO term and 0 signifies that it is not) was built. Subsequently, for all possible pairs the Jaccard's distance was calculated to generate a symmetric GO adjacent matrix. The dynamicTreeCut algorithm was employed to identify clusters of similar GO terms and the top 20% highest edges were selected for plotting. The highest scoring node within each cluster was designated as the cluster label (rName). The resulting nodes and network files were imported into Cytoscape (v 3.8.0) for network organization and visualization, as previously described.[58] For overrepresentation analysis (ORA) of GO terms DEGs, PANTHER was employed as classification system.[53]

Identification of HKG candidates in refined and standard EwS culture conditions

To identify suitable HKG candidates with a stable expression across culture techniques and EWSR1::ETS expression levels, the approach described by de Jonge et al.[34] was adapted as follows: All genes retrieved after joint background correction, normalization, summarization, and annotation (as described above) were filtered for a maximum |log2FC| <2, with the maximum FC defined as the maximum minus the minimal gene expression value across all samples for each gene. Subsequently, all filtered genes were ranked according to their coefficient of variation (CV = standard deviation/mean). The genes with the smallest CV were considered top HKG candidates (see also Table S4).

QUANTIFICATION AND STATISTICAL ANALYSIS

Statistical analysis and software

Statistical data analysis was performed using PRISM 10 software (GraphPad Software Inc., Ca, USA) or R (version 4.3.0) on the raw data. Two groups in functional *in vitro* experiments were compared with a two-sided Mann-Whitney test, if not indicated otherwise in the figure legends. Data are displayed as dot plots with vertical bars representing means and whiskers representing the standard error of the mean (SEM), if not indicated otherwise in the figure legends. Sample sizes for all *in vitro* experiments were chosen empirically. For generation of size proportional Venn diagrams, the DeepVenn web application was used.[43] Horizontal dashed lines in violin plots represent first and third quartiles (Q1, Q3) and solid lines the median.